



## Assessment of Characteristics and Performance of Fabricated Polysulfone and Polyethersulfone Hollow Fiber Membranes for Hemodialysis



S. R. Tewfik<sup>a</sup>, M. H. Sorour<sup>a</sup>, H. F. Shaalan<sup>a</sup>, H. A. Hani<sup>a\*</sup>, A. M. G. Abulnour<sup>a</sup>,  
M. A. Eltoukhy<sup>a</sup>, Y. O. A. Mostafa<sup>b</sup>, A.N. Mohamed<sup>a</sup>, M. A. M. Awad<sup>c</sup>

<sup>a</sup>Chemical Engineering and Pilot Plant Department, National Research Centre, Dokki, Giza, Postal code 12622, Egypt

<sup>b</sup>Mechanical Engineering Department, National Research Centre, Dokki, Giza, Postal code 12622, Egypt

<sup>c</sup>Clinical Pathology Department, National Research Centre, Dokki, Giza, Postal code 12622, Egypt

### Abstract

Hemodialysis is a common treatment method for chronic renal failure, where the dope composition and spinning parameters significantly influence the hemodialysis hollow fiber (HDHF) membrane characteristics and separation performance. This study investigates the performance and characteristics of HDHF membranes due to planned variations of dope composition and spinning parameters. The membranes were prepared on a semi-pilot scale experimental set-up. All fibers were characterized using scanning electron microscopy, atomic force microscopy, porosity and pore size assessment, mechanical properties, zeta potential, and performance evaluation. The fibers exhibited a double-layer finger-like structure with thickness between 208 and 264  $\mu\text{m}$  and pure water flux ranging from 3 to 22  $\text{L}/\text{m}^2\cdot\text{h}\cdot\text{bar}$ . Membranes prepared from polyethersulfone showed the lowest roughness (16nm) and the highest break stress and exhibited low flux values classifying them as low-flux hemodialysis membranes. In contrast, those made from polysulfone demonstrated higher flux values which are suitable for high-flux hemodialysis applications. Protein adsorption and platelet adhesion results were similar to those of commercial hemodialysis membranes. It is important to note that the thicker walls of the HDHF membranes did not negatively impact their characteristics and performance. The study offers insights into optimal conditions for fabricating HDHF membranes across various flux classes.

**Keywords:** hollow fiber membranes; hemodialysis; Polysulfone; Polyethersulfone; characteristics; performance

### 1. Introduction

Hemodialysis is a blood purifying treatment that removes toxins and extra water from the blood, as well as regulates blood electrolytes [1,2]. During dialysis, a patient's blood is pumped from an artery to a dialysis machine and then back to a vein in a closed continuous circuit. In the machine, the blood enters a hollow fiber dialyzer, provided with fibers of small pores. On the other side of these fibers flows counter currently a dialysate formed of acetate- or bicarbonate-based solution [3]. In standard dialysis treatment, water and solutes migrate according to concentration and pressure gradients as blood passes through the dialyzer [4]. The purified blood is then returned back to the patient.

Uremic retention compounds are classified into three categories: small solutes with upper molecular weight limit of 500 Daltons, middle molecules ranging from 500 to 60,000 Daltons, and protein-bound toxins. Compounds comprising the first category possess a high degree of water solubility and minor protein binding. The second category is highly synonymous with peptides and proteins that accumulate in uremia [5]. Small molecules can be removed by any dialysis membrane through diffusion, while middle molecules can be removed by dialyzer membranes by convection [2]. The final category has high affinity for binding with other uremic toxins. Protein-bound uremic toxins are associated with increased cardiovascular and mortality risks; however, their elimination is difficult during hemodialysis [6]. Dialyzers must therefore be able to remove a significant amount of middle-molecule-sized uremic toxins, while loss of vital proteins such as albumin must be restricted [7].

The hemodialysis hollow fiber (HDHF) membrane should be of high selectivity and hemocompatibility [8]. Essential characteristics governing the effectiveness of HDHF membrane include the morphology of the cross section and surface of membranes, elemental composition, surface roughness, hydrophilicity and mechanical characteristics. HD membrane should be of high hydrophilicity, high porosity, low surface roughness, decreased negative surface charge, high mechanical strength, and stability.

The dry-wet phase inversion process is the most often studied technique for creating HDHF. Crucial spinning parameters have been provided in several publications [9–13]. These include the dope composition and its effect on viscosity, spinneret

\*Corresponding author e-mail: [hi\\_heba2@yahoo.com](mailto:hi_heba2@yahoo.com); (Heba A. Hani).

Receive Date: 10 December 2024, Revise Date: 22 January 2025, Accept Date: 09 February 2025

DOI: 10.21608/ejchem.2025.343407.10958

©2025 National Information and Documentation Center (NIDOC)

dimensions, bore flow rate versus dope flow rate, bore fluid composition, drawing speed, air gap distance and temperatures of coagulation, block, and washing baths.

Dope composition and spinning parameters have a strong effect on hemodialysis membrane characteristics, thus morphology, mechanical properties and separation performance could be tailored by variation of these parameters during the spinning process. To improve performance, several studies have also investigated post-treatments such as heating in hot water and air [9], and hypochlorite treatment for the fabricated fibers [14,15].

Fabrication of HF membranes for commercial hemodialysis dialyzers and/or for use in research, many polymers with different molecular weights are being employed such as polysulfone (PS), polyethersulfone (PES) and sulfonated PES [16]. Solvents such as dimethyl acetamide (DMAc) and N-Methyl-2-pyrrolidone (NMP) are most commonly used for HDHF. Several additives are added to the dope to provide specific characteristics. Some researchers have employed polyvinyl pyrrolidone (PVP) and/or polyethylene glycol (PEG) to increase hydrophilicity and act as a pore former [8–11,16–21].

The effect of PVP as dope additive was previously studied by Yang et al. [13]. The surface roughness of both the inner and outer surfaces is influenced by the PVP content in PES/PVP membranes. The molecular weight cut-offs MWCOs of PES/PVP HF membranes appear to be most suitable for use in hemodialysis when heat-treated at 150°C in air. Using PVP 90K has reduced the contact angle (CA) and improved the hydrophilicity of PES membranes. Additionally, the HF membranes' smooth, hydrophilic, and negatively charged inner surface, spun with PVP-360K as the additive, produces the highest hemofiltration performance with the least amount of protein adsorption and the greatest amount of Bovine serum albumin (BSA) retention. The majority of unblended PVP may be effectively removed from the membrane matrix using the NaOCl bleaching procedure, thus reducing the risk of PVP entering the body and preventing its buildup in internal organs.

The main objective of this work is to investigate the performance and characteristics of HDHF due to planned variations of dope composition and spinning parameters. Emphasis has also been placed on the dependence of related transport properties on wall thickness and surface roughness as compared to commercial HDHF membranes. Fibers morphology, composition, surface roughness and other variables have been evaluated and compared. Performance represented by pure water permeability, urea and creatinine rejection and protein adsorption have been measured and analyzed.

## 2. Experimental

### 2.1. Materials

Polyethersulfone (PES) flakes (Ultrason E6020 D; MW 50,000 g/L) and polysulfone (PS) pellets also supplied from (BASF, Germany) were used as the base polymers. N-methyl-2-pyrrolidone (NMP) and dimethylacetamide (DMAc) supplied from Carl-Roth and Merck, respectively were used as solvents. Poly(vinyl pyrrolidone) (PVP) from Sigma-Aldrich and polyethylene glycol (PEG) from Merck were used as additives. Reverse osmosis (RO) water was used in the bore fluid, coagulation and washing bath media. Glycerol 99% and formaldehyde solution have been purchased from Fisher Scientific and Biochem, respectively. Urea and creatinine were purchased from El-Nasr Pharmaceutical Chemicals Co. and Alpha Chemicals Co. respectively. Bovine serum albumin (BSA) for protein adsorption experiments was purchased from Sigma Aldrich. Glutaraldehyde solution 50% was purchased from Alpha Chemica and phosphate buffered saline (PBS) was purchased from Biowest. These were used for the platelet adhesion test, where platelet-rich plasma (PRP) was prepared in the Clinical Pathology Laboratory at the National Research Centre from freshly withdrawn human blood from volunteers, as mentioned in details in section 2.3.4.

### 2.2. Fabrication and characterization of HDHF membranes

#### 2.2.1. HDHF Membranes Fabrication

Experiments for HDHF membranes fabrication have been conducted by dry-wet phase inversion method to form integrally skinned asymmetric membranes. These experiments enable the identification of optimum conditions for various parameters including dope and bore composition and spinning parameters. Experiments were undertaken on the semi-pilot spinning line. Detailed experimental set-up and procedure are described elsewhere. [22] The solvent is fed into the agitated jacketed reactor heated to 60-80°C. The polymers adopted were PS or PES which have been vacuum-dried for 8-10 hours and were gradually added to the solvent until complete dissolution. Since these polymers are hydrophobic, additives such as PVP or PEG, were added to improve hydrophilicity in addition to being pore formers. After complete homogenization of the dope by thorough mixing for 48 hours at least, the dope is pumped to pass through the block containing spinnerets with inner and outer diameters of 110 µm and 1000 µm, respectively.

The block temperature is controlled by a heat exchanger. Simultaneously the bore fluid which is RO or a mixture of water and solvent (NMP) is pressurized through the spinneret's needles at a specified flow ratio to the dope. The semi-formed fibers from the spinnerets fall through an adjusted air gap distance into the coagulation bath (RO water). The fibers from the coagulation bath pass through adjustable tension units to two consecutive RO water baths (average temperatures 18-25 °C) and are then directed to a reel winder.

Spun fibers were washed for two days in RO water followed by post treatment by immersion in aqueous glycerol for 1 hour then stored in formalin. Table 1 depicts the dope compositions, corresponding viscosities, and the main operating conditions of selected samples from several experiments conducted within the scope of this work. Every sample was prepared repeatedly for 2-5 times for reproducibility.

**Table 1: Selected dope composition and main spinning conditions\***

Sample code	A	B	C	D
<b>Polymer</b>	PS	PS	PS	PES
<b>Additives</b>	PVP	PEG	PVP	PVP
<b>Solvent</b>	NMP	NMP	DMAc	NMP
<b>Viscosity (cP)</b>	4,250	3,500	3,075	20,600
<b>Bore fluid</b>	RO:NMP	RO:NMP	RO:NMP	RO
<b>Air gap (cm)</b>	10	25	25	15

\*PS: polysulfone, PES: polyethersulfone, PVP: polyvinylpyrrolidone, PEG: polyethylene glycol, NMP: N-Methyl-2-pyrrolidone, DMAc: Dimethylacetamide, RO reverse osmosis purified water

### 2.2.2. HDHF Membranes Characterization

Membrane characteristics, such as morphology, roughness, mechanical properties and porosity and parameters defining the interaction of membranes with species in feed solutions, such as hydrophilicity, surface charge and zeta potential may be used to categorize factors affecting the membrane's performance [23–25]. The following characteristics have been determined for fabricated HDHF samples. For all characterization techniques, a minimum of 5 fibers were studied with several measurements for each sample and their average values were calculated.

#### Morphology

The morphology of the HDHF membranes was studied through Scanning electron microscope (SEM) images were obtained using JEOL SEM 6000 Neoscope desktop. HDHF samples were cut using a sharp razor, gold-sputtered, and then fixed on the sample stage using carbon double-faced tape [26–29]. Morphological structures of HFDF, inside and outside diameter, as well as, wall thickness were determined.

#### Surface roughness

HDHF membranes surface roughness was analyzed using 1.5 micron resolution TT-atomic force microscope (AFM), equipped with a video optical microscope with up to 400X zoom. A one-cm-long fiber sample was fixed using a double-faced tape on the magnetic plate of the AFM apparatus. Vibrating scan mode was used for testing a scan area of 5µm×5µm. Roughness parameters were calculated using “Gwyddion” software [26–29].

#### Mechanical properties

Mechanical properties of HDHF samples were studied using a benchtop tensile testing machine, Tinius Olsen H5kS, equipped with a 5N load cell. Testing was undertaken at 50 mm/min speed and a gauge length of 100 mm [26–29]. Tensile strength, elongation at break and fibers' Young's modulus were measured.

#### Porosity

The porosity of the fibers was measured using the gravimetric method according to the procedure described previously [12] by measuring the weight of the liquid entrapped within the membrane pores. The overall porosity of the fiber membrane ( $\epsilon$ ) was calculated using the following formula [22,26,30] :

$$\epsilon(\%) = \frac{\frac{(W_2 - W_1)}{Dk}}{\frac{(W_2 - W_1)}{Dk} + \frac{W_2}{D_{pol}}} \times 100 \quad (1)$$

where  $w_1$  is the weight of the dry membrane,  $w_2$  the weight of the wet membrane,  $Dk$  is the density of kerosene oil (0.82 g/cm<sup>3</sup>),  $D_{pol}$  is the density of polymer composite (PES and PS) (1.336 g/cm<sup>3</sup>).

#### Water contact angle (CA)

The hydrophilicity of the fibers was evaluated by measuring their contact angles. The water contact angle (CA) of the HF membrane was measured on an Attention Theta optical contact angle instrument (KSV Instruments Ltd) through a digital video image of the water drop of 5 µL volume on the dried surface of the hollow fiber at 25°C. [26–29]. All the samples were tested at five different positions and the final results presented are an average of the measured values.

#### BET analysis

Mean pore size and Brunauer-Emmett-Teller (BET) surface area for the prepared HDHF membrane samples were determined using the pore size distribution analyzer Belsorp Max apparatus (MicrotracBel. Corp.). Adsorptive nitrogen was used at 77 K. The Vacuum degree before the measurement was 6.95E-4 Pa and the standard vapor pressure was 108 kPa [26,28,29].

#### Zeta potential

The surface charges of the HDHF membranes were measured on SurPASS electrokinetic analyzer (Anton-Paar GmbH, Austria) [26,31]. Samples were cut by a razor, and then fixed to the sample holder using double-sided glue to be completely covered with flattened fibers. The channel height was 110 ± 5 µm. Liquid KCl (10 mM) was used as an electrolyte solution. The pH value of the solution was adjusted between 3-and 8.5 using an automatic titrator. The zeta potential was then calculated from the obtained streaming potential using the Helmholtz-Smoluchowski equation [32]:

$$\zeta = \frac{\eta K_B}{\epsilon_0 \epsilon_r} \left( \frac{dE_z}{d\Delta p} \right) \quad (1)$$

Where  $\zeta$  is the zeta potentia (V),  $\eta$  is the viscosity (Pa·s),  $K_B$  is the conductivity of electrolyte solution (S/m),  $\Delta p$  is the trans-membrane pressure (bar),  $\epsilon_0$  is the permittivity (C/(V·m)),  $\epsilon_r$  is the permittivity (C/(V·m)), and  $dE_z$  is the electrical potential drop (V).

### 2.3. Performance Evaluation

#### 2.3.1. Pure Water Permeability (PWP)

Performance tests were conducted using an apparatus for permeability testing: Hyflux Evaluation System. The schematic flow sheet is represented in Fig. 1. utilizing in/out mode.

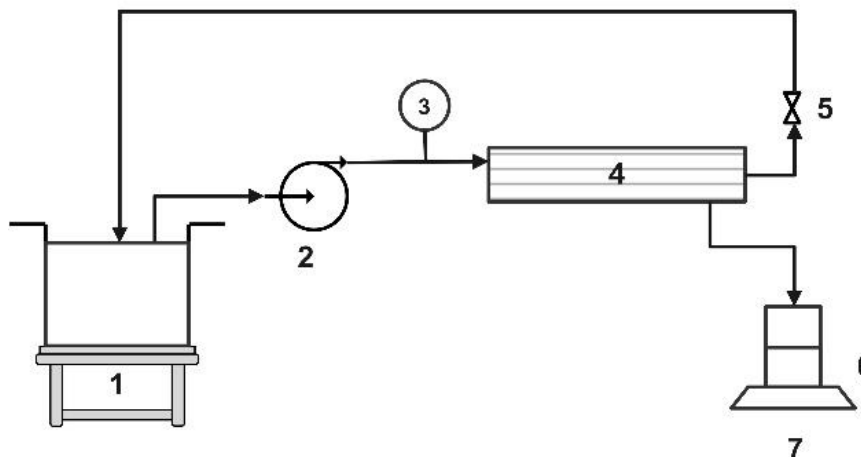


**Fig. 1. Schematic flow sheet of Hyflux system, where: 1. Feed/retentate reservoir, 2. Feed pump, 3. Pressure gauge, 4. Membrane glass module, 5. Valve, 6. Permeate collector**

$$PWP = \frac{V}{A \cdot t \cdot \Delta p} \quad (3)$$

Where: PWP is the pure water permeability rate (Lm<sup>-2</sup>h<sup>-1</sup>), V is the permeation volume of water (L), A is the effective membrane area (m<sup>2</sup>) and t is the sampling time (h), and  $\Delta p$  is the trans-membrane pressure (bar).

#### 2.3.2. Sieving Coefficient

Urea and creatinine were used to represent small toxins in the blood. All separation experiments were performed using the apparatus illustrated in Fig. 1. under constant transmembrane pressure (TMP) at room temperature. Solutions containing urea (300-1000 ppm) and creatinine (60-150 ppm) were prepared. All solutions were prepared in 0.9% sodium chloride saline solution. Permeate samples were collected after 30 minutes from the beginning of the operation, to ensure stability, then hourly up to 3 hours [26]. The concentrations of urea and creatinine were analyzed using ultraviolet–visible (UV-Vis) spectrophotometry. The sieving coefficient is calculated from equation (4).

$$SC = \frac{C_p}{C_f} \quad (4)$$

Where SC is the sieving coefficient  $C_f$  and  $C_p$  are the feed and permeate concentrations respectively

#### 2.3.3. Protein Adsorption

Albumin adsorption experiments were performed in static mode according to Santos et al. 2019 [33]. Fibers of each sample (100 mg) were cut into a length of approximately 1 cm. The fibers were rinsed in 0.9% NaCl solution for 1 day. The fibers were then filtered and immersed in 200 mL of BSA solution (4 g/L). Adsorption experiments were conducted at 37 °C under shaking for 2 h.

The amount of albumin adsorbed, in mg of albumin per mg of HF membrane, was determined according to equation (5)

$$\text{Protein adsorption} = \frac{(m_i - m_f)}{m_{\text{membrane}}} \quad (5)$$

where  $m_i$  is the initial quantity of albumin in solution,  $m_f$  is the quantity of albumin in solution after the time of contact with the membrane and  $m_{\text{membrane}}$  is the quantity of membrane packed in glass tubes.

#### 2.3.4. Platelet Adhesion

Platelet adhesion studies were performed using platelet-rich plasma (PRP) according to published work [34–36]. Platelet-rich plasma was prepared in the Clinical Pathology Laboratory in the Medical Research Institute at the National Research Centre from freshly withdrawn blood samples (10 ml) from two volunteers. Informed consent was obtained from all volunteers.

All experiments have been performed in accordance with relevant guidelines and regulations prevailing ethical and medicolegal framework governing the use of human blood from volunteers. The Medical Research Ethics Committee in the National Research Centre has approved this work (Approval no. 13410224) where the relevant Egyptian laws and the Egyptian Drug Authority (EDA), Ministry of Health and Population (MOHP) and Institutional Animal Care and Use Committee (IACUC) decrees, guidelines and recommendations were adopted and followed during the conduction of this research.

Eight fibers (1.5 cm) were opened longitudinally and immersed in a phosphate buffer saline (PBS) solution for 1 hour at 37°C. After that, the solution was removed and 1 ml of fresh PRP was introduced to the membrane. The membrane was then incubated with PRP at 37°C for 2 hours. This was then followed by PRP decantation, and the membrane was rinsed with PBS and treated with 2.5 wt. % glutaraldehyde in saline for 2 days at 4°C. It was then washed with PBS solution and subjected to a drying process through a series of graded alcohol-saline solutions. The dried membrane was examined using SEM to compare the number of adhering platelets.

### 3. Results and Discussion

#### 3.1. HDHF Membranes Morphology

##### 3.1.1. SEM

The SEM images of the prepared HDHF samples (A, B, C, and D) have been obtained and presented in Fig. 2. illustrating i) cross-section of the fibers and ii) wall thickness of the fibers. As shown in Fig. 2, the fiber cross section is a well-formed circular/slightly oval lumen that exhibits an asymmetric structure. Cross-sectional images as illustrated reveal that HDHF samples are composed of a thin and dense skin layer and two finger-like porous structures with a spongy layer in between. The skin layer is responsible for permeating and retaining solutes, whereas the porous bulk acts as a mechanical support.

It was demonstrated that the assessed dope compositions and spinning parameters affected both pore structure and fiber diameters. Sample C showed the most regular porous structure with an inner spongy skin layer which was prepared using DMAc as solvent. A higher thickness intermediate layer appeared for sample B with lower inner and outer skin layer thickness. Both finger-like layers appeared longer in case of sample D prepared using PES as the main polymer.

Table 2 depicts the change in fiber dimensions obtained from SEM images. Sample B showed the lowest wall thickness among the studied membranes, while sample D showed the highest thickness. Also, a lower air gap resulted in increased membrane thickness for PS samples as appeared in sample A compared to samples B and C.

Table 2: Dimensions of the prepared HDHF samples

Property	A	B	C	D
ID (μm)	342	284	252	477
OD (μm)	800	701	679	972
Thickness (μm)	248	208	213	264

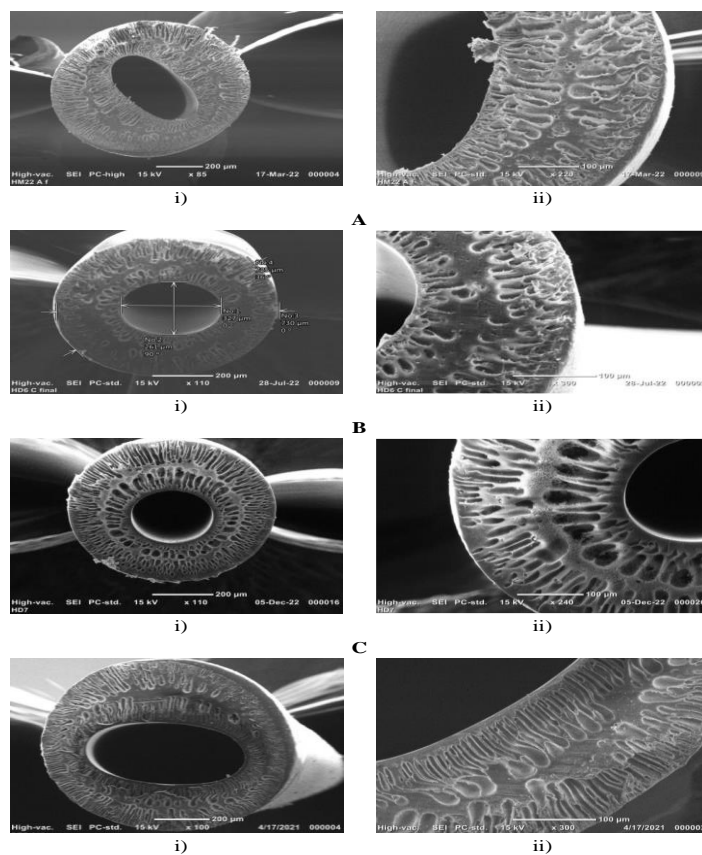


Fig. 2. SEM images of HDHF samples

### 3.1.2. AFM

The AFM images of the prepared HDHF samples are presented in Fig. 3. The average surface roughness values ( $R_a$ ) for samples A, B, C and D are 47, 31, 24 and 16 nm, respectively. It was observed that membrane prepared using PES as base polymer (sample D) provides the lowest surface roughness when compared to membranes prepared from PS polymer. On the other hand, results showed that using PVP instead of PEG as dope additive at higher air gap resulted in reduced roughness.

It was reported that higher surface roughness results in increased protein adsorption and platelet adhesion which decreases membrane hemocompatibility [37,38]. Moreover, Increased surface roughness resulted in an increase in the shear stress experienced by red blood cells close to the membrane surface, which can lead to hemolysis [38].

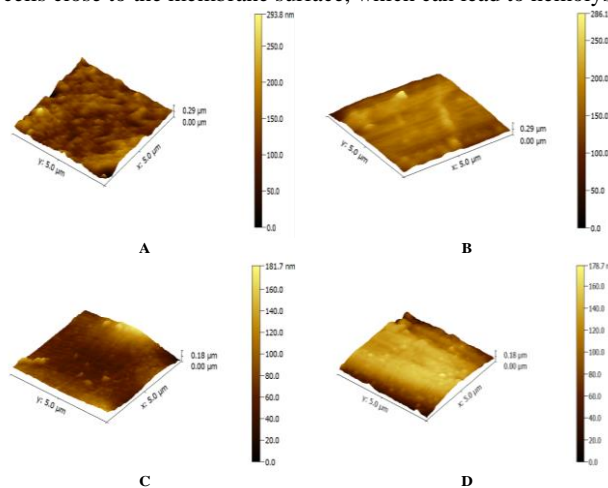


Fig. 3. AFM images of HDHF samples

Previously published work revealed that Lee and Hong reported surface roughness similar to our findings for PES/PVP flat sheet membranes. They also reported  $R_a$  varying between 29 and 45 nm depending upon the composition [39]. Also, Mansur et al., (2016) [19] reported mean surface roughness varying between 7.5 and 36 nm with increasing air gap distance from 3 to 100 cm. Also, for PES/PVP HF, Barzin et al. (2004) [9] reported outer surface roughness of 12.6 nm which decreased to 6 nm upon heat treatment for PES/PVP HF Membrane. Values as low as 3.55 for the inner surface have been reported by Verma et al.2018 [40].

Surface roughness of HF membranes is a critical factor in their performance for hemodialysis. It primarily affects the interaction of the membrane with blood and dialysate. Smoother surfaces reduce clotting and hence thrombosis [41]. Also, fouling sites increase with increased roughness leading to blood cells damage (biofouling) [42]. In addition, less turbulence is induced on smoother surfaces. Generally, in hemodialysis, the ideal membrane surface should be smooth enough to ensure biocompatibility and prevent fouling but tailored for optimal filtration and mechanical properties [43]. Accordingly, it can be deduced from our work that sample D, with the smoothest surface, is the most suitable for hemodialysis from roughness point of view.

It is worth mentioning that using PES increased the dope viscosity dramatically as compared to PS, which resulted in much lower surface roughness as shown in Sample D in Fig. 4.

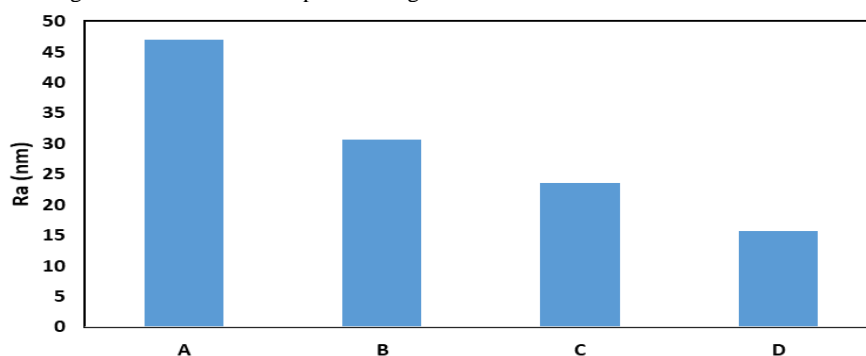
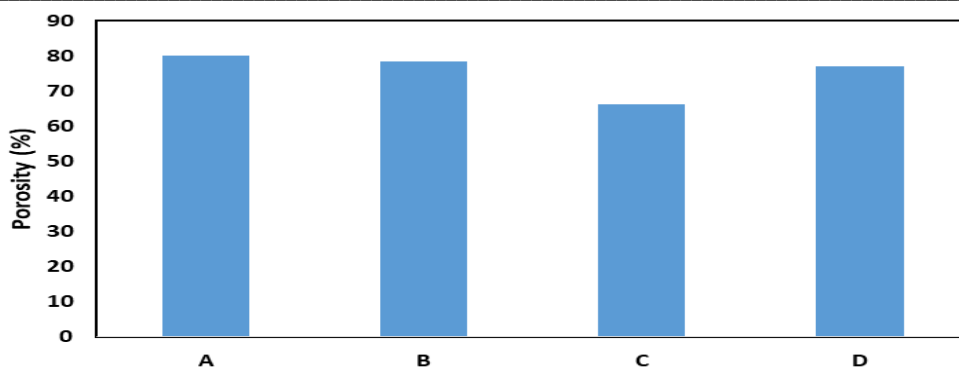


Fig. 4. Surface roughness of the prepared HDHF samples

### 3.1.3. Membranes Hydrophilicity

The surface contact angle of the prepared HDHF samples ranged from 68.3-75.6°, indicating hydrophilic surfaces, which is very similar to that reported by Mansur et al. [19]. It is worth mentioning that hydrophilicity is one of the most important parameters for HD membranes. It improves the permeability and biocompatibility of the membrane by inhibiting the adhesion of proteins or platelets[39]. As depicted in Fig. 5., DMAc gave the lowest porosity for the same sample C as compared to samples with NMP as solvent.



**Fig. 5. Average porosities of the prepared HDHF samples**

### 3.2. HDHF Membranes Porosities

The porosities of the prepared HDHF samples determined by the gravimetric method are in the range of 66-80% which is close to the range of 60-70% reported by Mansur et al. [19]. Said et al. (2017) [20] reported porosities for PS/PVP HF of 17.6 to 46% for air gap 3 to 50 cm which are much lower than our results. However, An et al. [44] prepared PVDF/PVDF-g-PACMO HF for hemodialysis. Their investigations deduced porosities similar to our results in the range of 67-89% depending on the PVDF to PVDF-g-PACMO ratio. This porosity range is preferred for hemodialysis membrane for enhanced toxins removal [45].

### 3.3. HDHF Membranes Mechanical Properties

Dialysis membranes should have good mechanical properties [2]. The mechanical properties were evaluated to indicate mechanical stability during processing and use [46] and they are presented in Table 3. High thickness finger- like supporting layer resulted in improved mechanical stability for prepared membranes. It is noticed that the lowest mechanical properties were obtained for sample C in which the solvent was DMAc. While sample A showed the highest tensile modulus at 188 MPa and sample B showed the highest break strain at 47.5%. Also, using PES (sample D) resulted in good mechanical properties as compared to samples A and B prepared from PS showing the most favourable mechanical properties in our work due to its high tensile stress, acceptable modulus and strain which will provide a mechanically stable membrane. Increasing air gap from 10 to 25 resulted in decreased break stress and break strain which may be attributed to decreased membrane thickness. It is clear that PEG as an additive (Sample B) increased the break strain, as shown in Table 3 when compared to other samples where the additive was PVP. DMAc as solvent gave the lowest mechanical properties in Sample C as compared to NMP in the three other samples.

HFHD mechanical properties are an indication of the membranes' reliability and durability during their lifetime [47,48]. High tensile stress is essential for preventing the fibers from breakage during dialysis process due to pressures and blood flow as well as ensuring ease of handling during assembly of dialysis modules [2,49]. Also, elongation at break permits the fibers to elongate without failure or breakage. At the end, good mechanical properties are crucial for patients' safety to evade membrane failure during operation [46,50].

**Table 3: Mechanical properties of the prepared HDHF samples**

	A	B	C	D
Break stress (MPa)	6.7	5.47	3.1	7
Break strain (%)	31.4	47.5	19.7	38
Young's modulus (MPa)	188	150	78.2	170

### 3.4. BET results

The measured mean pore diameter, BET surface area and total pore volume for selected samples (B and C) are listed in Table 4. It is apparent that there is a minor increase in the pore size from 5.03 to 6.87 nm between B and C membranes, corresponding to the change of solvent. These results are confirmed by the porosity range (65-78%). In addition, the presence of finger-like pores and the formation of sponge-like structure in SEM images of samples B and C confirm the minor change in pore size. These results are in agreement with reported dialysis hollow fiber membrane pore radii ranging between 2 and 10 nm according to Vienken J [51]. Typically, a high flux dialysis membrane mean pore size is in the range of 5–10 nm [52].

**Table 4: Mean pore diameter, BET surface area and total pore volume of HDHF samples**

Sample	Mean pore diameter (nm)	BET surface area (m <sup>2</sup> /g)	Total pore volume (cm <sup>3</sup> /g)
B	5.03	41.9	5.27E-2
C	6.87	86.5	0.1476

### 3.5. Zeta Potential

Zeta potential charts for selected samples (B and C) are presented in Fig. 6. It is clear that sample B (prepared using PEG) reveals higher negativity than sample C. The latter showed a stable charge over the pH range studied. Low surface charge results in decreased protein adsorption and thus higher hemocompatibility [53].

Thus, sample B is considered more suitable for hemodialysis application. However, tested membranes showed acceptable surface charge based on commercial membranes characteristics [54].

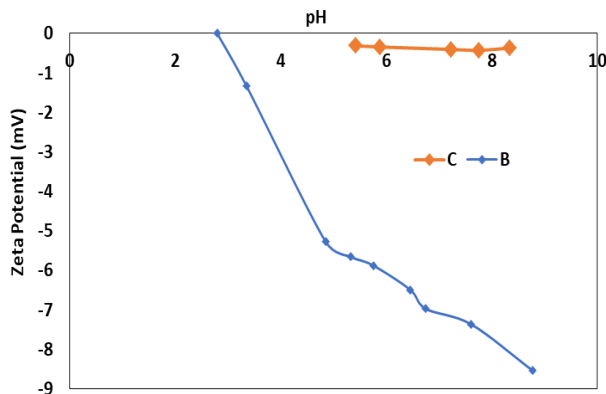


Fig. 6. Zeta potential for HDHF samples

Hemodialysis membranes have to be negatively charged to prevent adhesion of negatively charged protein blood and blood coagulation. The current trend in HD membrane development is to create near-zero charged surfaces to minimize any possible electrostatic interaction with human serum proteins or other molecules whose adsorption can provoke further cascade reactions and related undesired consequences [55].

### 3.6. Performance Analysis

#### 3.6.1. Pure Water Permeability

The pure water flux experiments were conducted using Hyflux apparatus utilizing in/out mode. Results are presented in Fig. 7. It is clear that sample (B) reveals the highest  $L/m^2.h.bar$  among the PS membranes which is in agreement with the range obtained from ASAHI PSF commercial membranes ( $27-31 L/m^2.h.bar$ ) (see Supplementary Table S1) in which typical characteristics of some commercial membranes are compiled and presented for completion. The results are also supported by the zeta potential results, where sample B processes the highest negativity. The water flux of the PES-prepared HDHF sample (sample D) is much lower than those reported by commercial companies such as Fresenius, Toray and Nipro which range between  $8-59 L/m^2.h.bar$ .

The two main categories of dialysis membranes available today are low and high flux. High-flux membranes can be classified into three main categories: (i) standard high-flux membranes that are currently in widespread use; (ii) expanded range membranes, which can remove middle molecules with a higher molecular weight than standard high-flux membranes with negligible albumin loss; and (iii) protein-leaking membranes, which can also remove an expanded range of middle molecules with a higher molecular weight without the need for an external substitution fluid infusion, but with a considerable loss of albumin.[56]. Moreover, it is clear that for the PS samples, the PWP increases with increasing the air gap. This is in agreement with the work of Said et al. [20] who demonstrated that for an increase in air gap from 3 to 50 cm, there was a corresponding increase of PWP from about 8 to  $28 L/m^2.h$ . Sample D where the base polymer is PES performed differently.

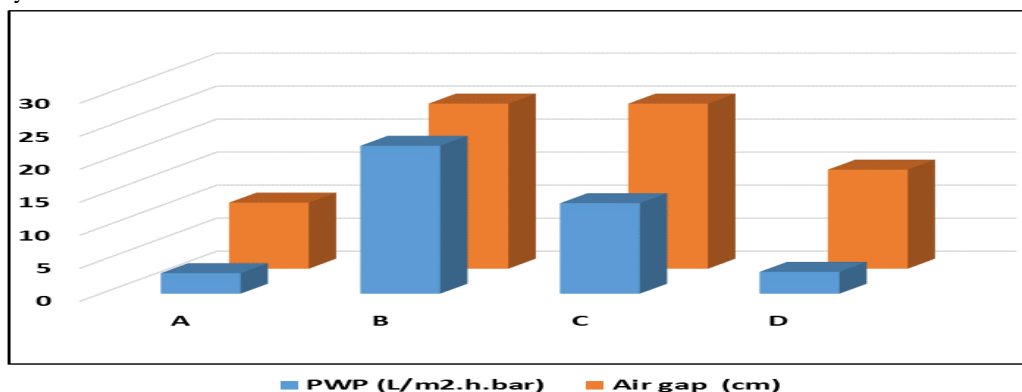


Fig.7. Effect of air gap on PWP for PS/PES HDHF samples



### 3.6.2. Sieving Coefficient

As shown in Table 5, sample A showed the highest sieving coefficient values for both urea (MW 62 Da) and creatinine at TMP 0.5 bar. Sample D also had acceptable values of urea and creatinine sieving coefficients under the same TMP. In other words, both samples can eliminate low molecular weight toxins and achieve the desired sieving coefficient, as the small toxins sieving coefficients for commercial hemodialysis membranes approach unity. On the other hand, sample B had the lowest value of the urea sieving coefficient at TMP 3 bar. Also, this sample could operate on ultrafiltration mode only at the aforementioned high working TMP. These results agree with previously published results reported by Lee et al. and Said et al. [39,57]. Thus, samples A and D are considered the best samples for urea and creatinine separation.

Table 5: Urea and creatinine sieving coefficients

Sample Code	Urea		Creatinine	
	1 <sup>st</sup> hr	2 <sup>nd</sup> hr	1 <sup>st</sup> hr	2 <sup>nd</sup> hr
A	0.924	0.995	0.94	1
B	0.73	0.9	Not Tested	
D	0.91	0.97	0.88	0.93

### 3.6.3. Protein Adsorption

Protein adsorption results, presented in Table 6, showed that sample D exhibited the highest value of 1.2 mg BSA/mg. Meanwhile, sample B showed the lowest protein adsorption value of 0.2 mg BSA/mg of the membrane. Thus, sample B is considered more suitable regarding protein adsorption. These results illustrated comparable protein adsorption to commercially available HD membranes PES (Baxter) and PS (Fresenius) having protein adsorption of 0.41 mg/mg and 0.20 mg/mg, respectively [33].

Table 6: Protein adsorption on HF membrane surface

Sample Code	Protein adsorption mg BSA/mg
A	0.8
B	0.2
D	1.2

### 3.6.4. Platelet adhesion

Static platelet adhesion experiments were performed for samples A and D based on promising separation performance results. SEM images of adhered platelets are shown in Fig. 8. It was observed that the number of platelets adhered to the inner membrane surface was clearly lower for sample D. The results indicate that sample D is less susceptible to thrombus formation, as platelet adhesion is an important factor for thrombus formation and coagulation, indicating higher biocompatibility.

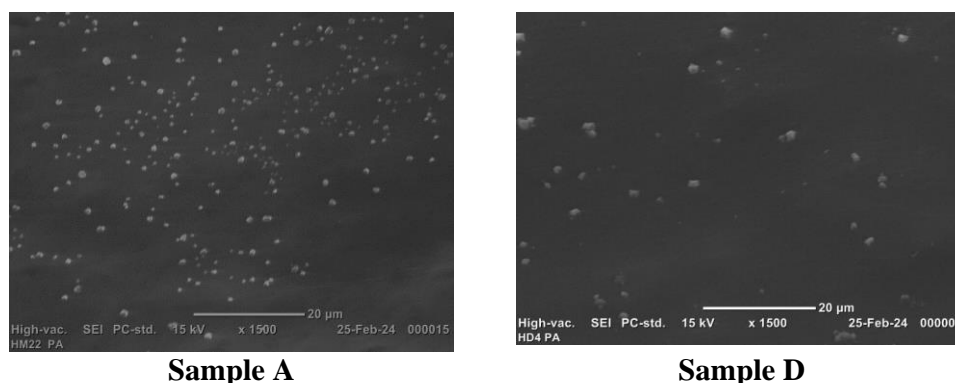


Fig. 8. SEM images for platelet adhesion for samples A and D

Performance results indicate comparable performance of the prepared HDHF membranes to commercial HDHF membranes having smaller wall thickness.

## 4. Conclusions

Adjustment of hemodialysis membrane characteristics is crucial for hemodialysis patients. In this work, planned variations in both dope composition and spinning parameters were studied to investigate their effect on membrane characteristics and separation performance. The results indicated that using polyethersulfone (PES) significantly increased dope viscosity compared to polysulfone (PS), leading to much lower surface roughness and decreased platelet adhesion. The addition of polyethylene glycol (PEG) improved the break strain compared to other additives. Additionally, when dimethyl

acetamide (DMAc) was used as a solvent, the membranes exhibited the lowest porosity and mechanical properties compared to membranes made with N-methyl-2-pyrrolidone (NMP). An increased air gap resulted in higher pure water permeability (PWP) for PS samples. The average surface roughness values (Ra) for the fabricated membranes ranged from 16 to 47 nm, where the lowest roughness was attributed to using the PES. The water contact angle varied between 68° and 76° and the porosity varied between 60% and 80%. The tested membranes displayed a low negatively charged surface, which is favorable for hemodialysis application. Pure water permeability was in the range of 3 to 22 L/m<sup>2</sup>·h·bar, aligning with different flux classes. Moreover, the protein adsorption and platelet adhesion to the membrane surface conformed to the typical characteristics of commercially standard types. It was concluded that thicker walls of the hemodialysis (HDHF) membranes did not adversely affect their characteristics and performance. This study provides insights into the optimal conditions for fabricating HDHF membranes across various flux classes. To further enhance the understanding and development of HDHF membranes, a comprehensive investigation of spinning conditions and dope compositions under a wider range of conditions should be systematically conducted.

#### Conflicts of interest

There are no conflicts to declare.

#### Formatting of funding sources

This work is funded by the Academy of Scientific Research and Technology, project: "Modification and quality improvement of currently prepared National Research Centre hollow fiber membranes for application in hemodialyzers".

#### Acknowledgments

The authors would like to thank the Ministry of International Cooperation for securing funds to support the Hollow Fibre Membranes Program at The National Research Centre from the Islamic Development Bank and Kuwait Fund for Arab Economic Development. This work is funded by Academy of Scientific Research and Technology and is titled "Modification and quality improvement of currently prepared National Research Centre hollow fiber membranes for application in hemodialyzers".

#### References

- [1] Sakai, K., 2000, "Dialysis Membranes for Blood Purification,," *Front Med Biol Eng*, **10**(2). <https://doi.org/10.1163/15685570052061973>.
- [2] Raharjo, Y., Abidin, M. N. Z., Ismail, A. F., Fahmi, M. Z., Saiful, Elma, M., Santoso, D., Haula', H., and Habibi, A. R., 2022, "Dialysis Membranes for Acute Kidney Injury," *Membranes (Basel)*, **12**(3). <https://doi.org/10.3390/membranes12030325>.
- [3] Baba, D., Gutti, B., and Zubairu, A., 2017, "Mathematical Modeling and Simulation of the Kidney Hemodialysis Modeling," *Faculty of Engineering Seminar Series*, pp. 18–24.
- [4] BagaRao, S., and Ghista, D. N., 2023, "Artificial Kidney Function and Dialysis Physiology: Mechanisms and Analysis of Hemodialysis and Peritoneal Dialysis," *Biomedical Engineering of Pancreatic, Pulmonary, and Renal Systems, and Applications to Medicine*. <https://doi.org/10.1016/B978-0-323-95884-4.00008-1>.
- [5] Clark, W. R., Deghani, N. L., Narsimhan, V., and Ronco, C., 2019, "Uremic Toxins and Their Relation to Dialysis Efficacy," *Blood Purif*, **48**(4), pp. 299–314. <https://doi.org/10.1159/000502331>.
- [6] Daneshamouz, S., Eduok, U., Abdelrasoul, A., and Shoker, A., 2021, "Protein-Bound Uremic Toxins (PBUTs) in Chronic Kidney Disease (CKD) Patients: Production Pathway, Challenges and Recent Advances in Renal PBUTs Clearance," *NanoImpact*, **21**, p. 100299. <https://doi.org/10.1016/J.IMPACT.2021.100299>.
- [7] Mollahosseini, A., Abdelrasoul, A., and Shoker, A., 2020, "Challenges and Advances in Hemodialysis Membranes," *Advances in Membrane Technologies*. <https://doi.org/10.5772/intechopen.90643>.
- [8] ter Beek, O. E. M., Pavlenko, D., and Stamatialis, D., 2020, "Hollow Fiber Membranes for Long-Term Hemodialysis Based on Polyethersulfone-SlipSkin™ Polymer Blends," *J Memb Sci*, **604**, p. 118068. <https://doi.org/10.1016/J.MEMSCI.2020.118068>.
- [9] Barzin, J., Feng, C., Khulbe, K. C., Matsuura, T., Madaeni, S. S., and Mirzadeh, H., 2004, "Characterization of Polyethersulfone Hemodialysis Membrane by Ultrafiltration and Atomic Force Microscopy," *J Memb Sci*, **237**(1–2), pp. 77–85. <https://doi.org/10.1016/j.memsci.2004.02.029>.
- [10] Su, B., Fu, P., Li, Q., Tao, Y., Li, Z., Zao, H., and Zhao, C., 2008, "Evaluation of Polyethersulfone Highflux Hemodialysis Membrane in Vitro and in Vivo," *J Mater Sci Mater Med*, **19**(2), pp. 745–751. <https://doi.org/10.1007/s10856-007-3006-9>.
- [11] Yin, Z., Su, B., Nie, S., Wang, D., Sun, S., and Zhao, C., 2012, "Poly (Vinylpyrrolidone-Co-Acrylonitrile-Co-Vinylpyrrolidone) Modified Polyethersulfone Hollow Fiber Membranes with Improved Blood Compatibility," *Fibers and Polymers*, **13**(3), pp. 269–276. <https://doi.org/10.1007/s12221-012-0269-7>.
- [12] Hasegawa, T., Iwasaki, Y., and Ishihara, K., 2002, "Preparation of Blood-Compatible Hollow Fibers from a Polymer Alloy Composed of Polysulfone and 2-Methacryloyloxyethyl Phosphorylcholine Polymer," *J Biomed Mater Res*, **63**(3), pp. 333–341. <https://doi.org/10.1002/jbm.10210>.
- [13] Yang, Q., Chung, T. S., and Weber, M., 2009, "Microscopic Behavior of Polyvinylpyrrolidone Hydrophilizing Agents on Phase Inversion Polyethersulfone Hollow Fiber Membranes for Hemofiltration," *J Memb Sci*, **326**(2). <https://doi.org/10.1016/j.memsci.2008.10.008>.

- [14] ThomINETTE, F., Farnault, O., Gaudichet-Maurin, E., Machinal, C., and Schrotter, J. C., 2006, "Ageing of Polyethersulfone Ultrafiltration Membranes in Hypochlorite Treatment," *Desalination*, **200**(1–3), pp. 7–8. <https://doi.org/10.1016/J.DESAL.2006.03.221>.
- [15] Dibrov, G., Kagramanov, G., Sudin, V., Grushevenko, E., Yushkin, A., and Volkov, A., 2020, "Influence of Sodium Hypochlorite Treatment on Pore Size Distribution of Polysulfone/Polyvinylpyrrolidone Membranes," *Membranes (Basel)*, **10**(11). <https://doi.org/10.3390/membranes10110356>.
- [16] Kaleekkal, N. J., Thanigaivelan, A., Tarun, M., and Mohan, D., 2015, "A Functional PES Membrane for Hemodialysis - Preparation, Characterization and Biocompatibility," *Chin J Chem Eng*, **23**(7). <https://doi.org/10.1016/j.cjche.2015.04.009>.
- [17] Sinha, M. K., and Purkait, M. K., 2013, "Increase in Hydrophilicity of Polysulfone Membrane Using Polyethylene Glycol Methyl Ether," *J Memb Sci*, **437**, pp. 7–16. <https://doi.org/10.1016/j.memsci.2013.03.003>.
- [18] Wang, H., Yu, T., Zhao, C., and Du, Q., 2009, "Improvement of Hydrophilicity and Blood Compatibility on Polyethersulfone Membrane by Adding Polyvinylpyrrolidone," *Fibers and Polymers*, **10**(1), pp. 1–5. <https://doi.org/10.1007/s12221-009-0001-4>.
- [19] Mansur, S., Othman, M. H. D., Ismail, A. F., Sheikh Abdul Kadir, S. H., Kamal, F., Goh, P. S., Hasbullah, H., Ng, B. C., and Abdullah, M. S., 2016, "Investigation on the Effect of Spinning Conditions on the Properties of Hollow Fiber Membrane for Hemodialysis Application," *J Appl Polym Sci*, **133**(30). <https://doi.org/10.1002/app.43633>.
- [20] Said, N., Hasbullah, H., Ismail, A. F., Abidin, M. N. Z., Goh, P. S., Othman, M. H. D., Kadir, S. H. S. A., Kamal, F., Abdullah, M. S., and Ng, B. C., 2017, "The Effect of Air Gap on the Morphological Properties of PSf/PVP90 Membrane for Hemodialysis Application," *Chem Eng Trans*, **56**, pp. 1591–1596. <https://doi.org/10.3303/CET1756266>.
- [21] Raharjo, Y., Ismail, A. F., Dzarfan Othman, M. H., Rosid, S. M., Azali, M. A., and Santoso, D., 2021, "Effect of Polymer Loading on Membrane Properties and Uremic Toxins Removal for Hemodialysis Application," *Journal of Membrane Science and Research*, **7**(1), pp. 14–19. <https://doi.org/10.22079/JMSR.2020.119864.1321>.
- [22] Shadia R. Tewfik, Mohamed H. Sorour, H. F. S. and H. A. H., 2018, "Effect of Spinning Parameters of Polyethersulfone Based Hollow Fiber Membranes on Morphological and Mechanical Properties," *Membrane Water Treatment*, **9**(1), pp. 43–51. <https://doi.org/https://doi.org/10.12989/mwt.2018.9.1.043>.
- [23] Deshrnukh, S. S., and Childress, A. E., 2001, *Zeta Potential of Commercial RO Membranes: Influence of Source Water Type and Chemistry*. [Online]. Available: [www.elsevier.com/locate/desal](http://www.elsevier.com/locate/desal).
- [24] Tytkowski, B., and Tsihranska, I., 2015, *OVERVIEW OF MAIN TECHNIQUES USED FOR MEMBRANE CHARACTERIZATION*.
- [25] Ravichandran, S. R., Venkatachalam, C. D., Sengottian, M., Sekar, S., Subramaniam Ramasamy, B. S., Narayanan, M., Gopalakrishnan, A. V., Kandasamy, S., and Raja, R., 2022, "A Review on Fabrication, Characterization of Membrane and the Influence of Various Parameters on Contaminant Separation Process," *Chemosphere*, **306**. <https://doi.org/10.1016/j.chemosphere.2022.135629>.
- [26] Mohamed, A. N., Hani, H. A., Tewfik, S. R., Ettouney, R. S., and El-Rifai, M. A. E. H., 2024, "Effect of Microwave Treatment on Morphological and Separation Characteristics of Polysulfone Hemodialysis Hollow Fiber Membranes," *Egypt J Chem*, **0**(0), pp. 0–0. <https://doi.org/10.21608/ejchem.2024.298237.9880>.
- [27] Sorour, M. H., Hani, H. A., Shaalan, H. F., and El-Toukhy, M., 2021, "Fabrication and Characterization of Hydrophobic PVDF-Based Hollow Fiber Membranes for Vacuum Membrane Distillation of Seawater and Desalination Brine," *Egypt J Chem*, **64**(9), pp. 4815–4819. <https://doi.org/10.21608/ejchem.2021.68699.3500>.
- [28] Tewfik, S. R., Sorour, M. H., Shaalan, H. F., Hani, H. A., Abulnour, A. M. G., and Sayed, E. S., 2021, "Assessment of Interfacial Polymerization Modalities on the Performance of Polyaniline Doped Polyethersulphone Hollow Fiber Membranes," *J Appl Polym Sci*, **138**(21). <https://doi.org/10.1002/app.50485>.
- [29] Tewfik, S. R., Sorour, M. H., Shaalan, H. F., Hani, H. A., Abulnour, A. G., El Sayed, M. M., Mostafa, Y. O., and Eltoukhy, M. A., 2023, "Effect of Post-Treatment Routes on the Performance of PVDF-TEOS Hollow Fiber Membranes," *Membrane and Water Treatment*, **14**(2), pp. 85–93. <https://doi.org/10.12989/mwt.2023.14.2.085>.
- [30] Drioli, E., Ali, A., Simone, S., Macedonio, F., AL-Jlil, S. A., Al Shabonah, F. S., Al-Romaih, H. S., Al-Harbi, O., Figoli, A., and Criscuoli, A., 2013, "Novel PVDF Hollow Fiber Membranes for Vacuum and Direct Contact Membrane Distillation Applications," *Sep Purif Technol*, **115**, pp. 27–38. <https://doi.org/10.1016/j.seppur.2013.04.040>.
- [31] Sobolev, V. D., Filippov, A. N., Vorob'eva, T. A., and Sergeeva, I. P., 2017, "Determination of the Surface Potential for Hollow-Fiber Membranes by the Streaming-Potential Method," *Colloid Journal*, **79**(5), pp. 677–684. <https://doi.org/10.1134/S1061933X17050155>.
- [32] Yun-ren, Q., Chang, M., and Hong-qi, Y., 2009, "Characterization of Polysulfone Hollow-Fiber Ultrafiltration Membrane and Its Cleaning Efficiency by Streaming Potential and Flux Method," *J. Cent. South Univ. Technol*, **16**. <https://doi.org/10.1007/s11771-009-0033-3>.
- [33] Santos, A. M., Habert, A. C., and Ferraz, H. C., 2019, "Polyetherimide / Polyvinylpyrrolidone Hollow-Fiber Membranes for Use in Hemodialysis," *Brazilian Journal of Chemical Engineering*, **36**(04), pp. 1645–1652.
- [34] Sakthi Kumar, D., Fujioka, M., Asano, K., Shoji, A., Jayakrishnan, A., and Yoshida, Y., 2007, "Surface Modification of Poly(Ethylene Terephthalate) by Plasma Polymerization of Poly(Ethylene Glycol)," *J Mater Sci Mater Med*, **18**(9), pp. 1831–1835. <https://doi.org/10.1007/s10856-007-3033-6>.

- [35] Xiang, T., Lu, T., Xie, Y., Zhao, W. F., Sun, S. D., and Zhao, C. S., 2016, "Zwitterionic Polymer Functionalization of Polysulfone Membrane with Improved Antifouling Property and Blood Compatibility by Combination of ATRP and Click Chemistry," *Acta Biomater*, **40**, pp. 162–171. <https://doi.org/10.1016/j.actbio.2016.03.044>.
- [36] Koga, Y., Fujieda, H., Meguro, H., Ueno, Y., Aoki, T., Miwa, K., and Kainoh, M., 2018, "Biocompatibility of Polysulfone Hemodialysis Membranes and Its Mechanisms: Involvement of Fibrinogen and Its Integrin Receptors in Activation of Platelets and Neutrophils," *Artif Organs*, **42**(9), pp. E246–E258. <https://doi.org/10.1111/aor.13268>.
- [37] Westphalen, H., Abdelrasoul, A., and Shoker, A., 2021, "Protein Adsorption Phenomena in Hemodialysis Membranes: Mechanisms, Influences of Clinical Practices, Modeling, and Challenges," *Colloids and Interface Science Communications*, **40**. <https://doi.org/10.1016/j.colcom.2020.100348>.
- [38] Abdelrasoul, A., and Shoker, A., 2022, "Influence of Hydration Shell of Hemodialysis Clinical Membranes on Surrogate Biomarkers Activation in Uremic Serum of Dialysis Patients," *Biomedical Engineering Advances*, **4**, p. 100049. <https://doi.org/10.1016/J.BEA.2022.100049>.
- [39] Lee, G. T., and Hong, Y. K., 2022, "Manufacturing and Separation Characteristics of Hemodialysis Membranes to Improve Toxin Removal Rate," *Advances in Polymer Technology*, **2022**. <https://doi.org/10.1155/2022/2565010>.
- [40] Verma, S. K., Modi, A., Singh, A. K., Teotia, R., and Bellare, J., 2018, "Improved Hemodialysis with Hemocompatible Polyethersulfone Hollow Fiber Membranes: In Vitro Performance," *J Biomed Mater Res B Appl Biomater*, **106**(3), pp. 1286–1298. <https://doi.org/10.1002/jbm.b.33941>.
- [41] Mansur, S., Othman, M. H. D., Abidin, M. N. Z., Malek, N. A. N. N., Ismail, A. F., Kadir, S. H. S. A., Goh, P. S., Abdullah, M. S., and Asraf, M. H., 2022, "Dual-Layer Hollow Fibre Haemodialysis Membrane for Effective Uremic Toxins Removal with Minimal Blood-Bacteria Contamination," *Alexandria Engineering Journal*, **61**(12). <https://doi.org/10.1016/j.aej.2022.03.043>.
- [42] Bacal, C. J. O., Munro, C. J., Tardy, B., Maina, J. W., Sharp, J. A., Razal, J. M., Greene, G. W., Nandurkar, H. H., Dwyer, K. M., and Dumée, L. F., 2024, "Fouling during Hemodialysis – Influence of Module Design and Membrane Surface Chemistry," *Advanced Membranes*, **4**, p. 100100. <https://doi.org/10.1016/J.ADVMEM.2024.100100>.
- [43] Alanazi, H., Nour, M., and Hussain, M. A., 2020, "Surface Nano-Characterization of Dialysis Membranes for Quality Purpose," *Middle East Conference on Biomedical Engineering, MECBME*. <https://doi.org/10.1109/MECBME47393.2020.9265174>.
- [44] An, Z., Xu, R., Dai, F., Xue, G., He, X., Zhao, Y., and Chen, L., 2017, "PVDF/PVDF-g-PACMO Blend Hollow Fiber Membranes for Hemodialysis: Preparation, Characterization, and Performance," *RSC Adv*, **7**(43), pp. 26593–26600. <https://doi.org/10.1039/C7RA03366D>.
- [45] Nguyen, T. T., Fareed, H., Le-Thi, A. D., Nguyen-Thi, K. S., Jang, K., Seong Kim, C., Wan Kim, S., Seo, J., Yang, E., and Kim, I.